

# Low temperature crack propagation in an epoxide resin

J. M. SCOTT, G. M. WELLS, D. C. PHILLIPS  
*Materials Development Division, AERE, Harwell, UK*

The effects of temperature and testing rate on the fracture energies and modes of crack propagation of an epoxide resin cured with a range of amine curing agents have been determined. The simplest behaviour observed consisted of unstable crack propagation at high temperatures with a transition to stable crack growth at lower temperatures ( $\sim 0^\circ\text{C}$ ) followed by a further transition (at  $\sim -150^\circ\text{C}$ ) back to unstable crack growth at the lowest temperatures. More complicated series of transitions were also observed. The variation of the upper transition temperature with testing rate and cross-linking density is qualitatively what would be expected from a model of limited crack tip plasticity but the reasons for the lower temperature transition are unknown. Some observations of the effects on crack propagation mode of curing conditions and water are also reported.

## 1. Introduction

Crack propagation in glassy polymers can be either stable (continuous) or unstable (stick-slip). For those epoxide resins in which crack propagation is unstable at ambient and higher temperatures it has been shown that instability decreases with increasing test rate and decreasing temperature [1, 2]. This behaviour can be explained qualitatively by considering the effects of temperature and strain rate on the plasticity of the material at the crack tip, although a quantitative modelling of this process zone has not yet been achieved. Direct observations of the crack tip in epoxide resins at ambient temperatures has shown [1] that when failure occurs in a stick-slip mode the stationary crack which is initially sharp under low stress, gradually blunts as the stress rises. Eventually, when the crack tip is deformed to some relatively large crack tip radius, and relatively large crack opening displacement, a new sharp crack suddenly develops at the tip of the original crack and accelerating rapidly, propagates some distance into the material arresting when the available elastic energy is insufficient for further growth. The process is then repeated as the load rises again. The decrease of instability and the transition from unstable crack growth, which occurs on decreasing temperature or increasing strain rate, is due to the decreasing

ductility of the resin under the same conditions. The stress at the crack tip depends on the applied load and the crack tip radius. As load increases the stress increases but an increase in crack tip radius through plastic flow reduces the stress concentration. The less ductile the material the more difficult it is for the crack tip to deform and the less the required applied load before the stress at the crack tip can rupture bonds.

Although the factors governing the transition from stability are not yet fully understood, from an engineering point of view the transition is rather important. This transition may to some extent be regarded as a brittle-ductile transition, and in addition there is good reason for believing that it denotes a significant change in the static fatigue behaviour of the resin [3]. At temperatures below the transition, slow crack growth can occur over a range of stress intensity factors, while above the transition this does not appear to happen.

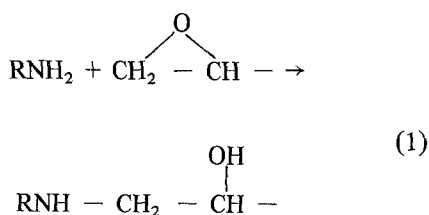
The original objectives of the present work were to investigate the way that this brittle-ductile transition is affected by factors such as the structure of the cured epoxide resin and testing rate, and in addition to extend measurements of fracture energy and observations of crack propagation modes to lower temperatures than previously studied. There is a need for such measurements

because of the important low-temperature uses of epoxide resins such as for insulating superconducting magnets and in space satellites. A surprising result of this work was the discovery of an unexpected further transition from stable to unstable crack growth at low temperatures. In addition, because of the well-known problems associated with obtaining reproducibility of epoxide data [1], some measurements were made of the effect of curing conditions on fracture energy in order to determine how sensitively they affected this property. These results and other observations of the effects of water are reported here because of their general interest.

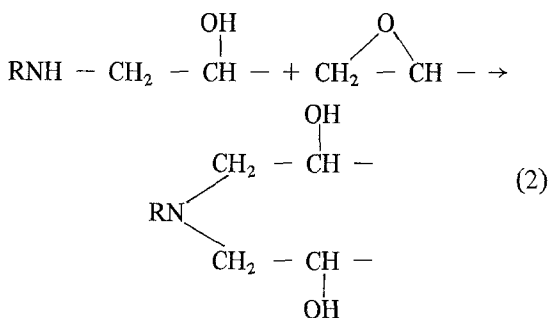
## 2. Experimental details

### 2.1. Preparation of material

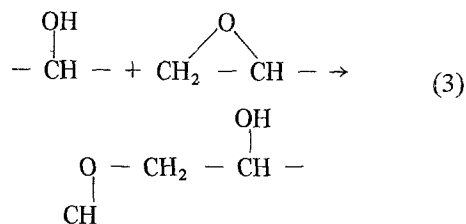
The epoxide resin used was Ciba-Geigy "Araldite" MY 750, a liquid diglycidyl ether of bisphenol A, with a molecular weight of approximately 360 and an epoxide content of 5.05 to 5.30 eq. kg<sup>-1</sup>. To eliminate the problem of batch variability, a single drum of resin was secured and only this resin used for the whole series of experiments. Four primary diamines were used as the hardeners — ethylene diamine, propane diamine, tetramethylene diamine and hexamethylene diamine (Table I). Cross-linking occurs by the reaction of an active hydrogen in the amine molecule with the oxygen atom in the epoxide group [4, 5].



The secondary amine so formed can react with another epoxide group.



An etherification reaction also occurs but only to a very limited extent:



The first and second reactions predominate, the former occurring at about twice the rate of the latter.

To manufacture plates, the resin was first degassed under vacuum for 20 min to remove dissolved air, and a stoichiometric proportion of liquid amine was then added and stirred for several minutes. EDA and PDA are liquids at room temperature but TDA and HDA have melting points of 27 and 42° C, and both amine and resin were raised above this temperature before mixing. After addition of curing agent the stirred mixtures were further degassed, but care was taken to ensure that a measured excess of amine had been previously added to compensate for the inevitable loss of some of the volatile amine. The mixture was cast in a steel mould previously baked with a silicon release agent. The standard cure schedule was 1 h at 60° C plus a postcure of 1 h at 160° C, these temperatures being controlled by four 800 W, disc-shaped, thermostatically controlled electrical heaters clamped to the sides of the mould. In this way,

TABLE I The curing agents

Curing Agent	Formula	Proportion (wt %)	Supplier
Ethylene diamine (EDA)	NH <sub>2</sub> (CH <sub>2</sub> ) <sub>2</sub> NH <sub>2</sub>	8.3	British Drug Houses Ltd
Propane diamine (PDA)	NH <sub>2</sub> (CH <sub>2</sub> ) <sub>3</sub> NH <sub>2</sub>	10.3	B. D. H. Ltd
Tetramethylene diamine (TDA)	NH <sub>2</sub> (CH <sub>2</sub> ) <sub>4</sub> NH <sub>2</sub>	12.2	Cambrian Chemicals Ltd
Hexamethylene diamine (HDA)	NH <sub>2</sub> (CH <sub>2</sub> ) <sub>6</sub> NH <sub>2</sub>	16.1	B. D. H. Ltd

T A B L E II Variation of physical properties with curing agent

Curing agent	Density ( $10^3 \text{ kg m}^{-3}$ )	"Barcol" impressor number	Glass transition temperature $T_g$ ( $^{\circ}\text{C}$ )
EDA	$1.1948 \pm 0.0012$	$29.4 \pm 1.8$	$128.0 \pm 2.4$
PDA	$1.1896 \pm 0.0010$	$26.0 \pm 1.5$	
TDA	$1.1847 \pm 0.0002$	$26.0 \pm 1.3$	$128.0 \pm 0.7$
HDA		$20.0 \pm 1.3$	$117.6 \pm 0.9$

bubble-free plates of dimensions  $255 \text{ mm} \times 160 \text{ mm} \times 3 \text{ mm}$  were produced for machining into specimens  $3 \text{ mm} \times 30 \text{ mm} \times 75 \text{ mm}$  for testing.

Problems were encountered at the beginning of the investigation with supposedly identical materials displaying different properties. A limited study was therefore made of the sensitivity of crack propagation to degree of cure and the results of this are described later.

## 2.2. Structural parameters

The reason for using the particular diamine hardeners selected was that they form a homologous series, each having the formula  $\text{NH}_2(\text{CH}_2)_n\text{NH}_2$ . Previous work has shown that the fracture energies of cast specimens of this epoxide resin cured with these different agents vary consistently with change in the molecular length of the curing agent [1]. Increasing the chain length of the curing agent (i.e. EDA–PDA–TDA–HDA) is expected to reduce the cross-link density and create a more open structure. Material parameters which might reflect this change were measured and Table II shows the variation of density, "Barcol" impressor number and glass transition temperature for the four systems. The Barcol impressor is a hand held instrument which presses a needle into the plastic surface giving a purely comparative measure of hardness. Densities were measured using a simple water immersion technique utilizing Archimedes' principle. Glass transition temperatures were determined using a differential scanning calorimeter. From the measurements it is clear that increasing the molecular length of curing agent gives a cured resin of lower density, reduced hardness and probably lower glass transition temperature.

## 2.3. Fracture energies

Fracture energies were measured by means of the double-torsion technique using pre-cracked specimens of dimensions  $3 \text{ mm} \times 30 \text{ mm} \times 75 \text{ mm}$ . This technique has been described fully elsewhere

[1] and will be only briefly summarized here. Fig. 1 shows schematically the specimen and test jig. By bending the end of a plate in three- or four-point loading a crack can be caused to run as shown. The main feature of this test geometry is that the specimen compliance  $C$  varies linearly with crack area  $A$ , So that by pre-calibrating the specimen to provide

$$\frac{\partial C}{\partial A}$$

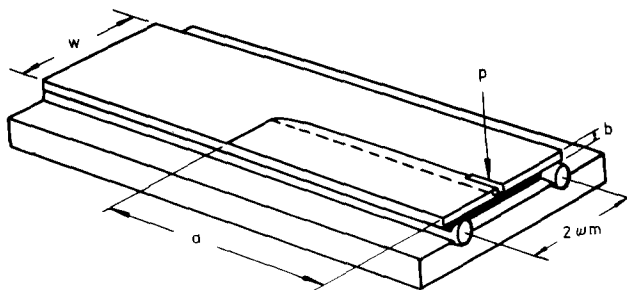
the fracture energy may be calculated from the crack propagation load,  $P$ , through the expression

$$G = \frac{P^2}{2} \frac{\partial C}{\partial A} .$$

Employing this technique, and depending on the testing conditions of temperature and strain rate, and material curing conditions, cracks either propagate continuously or in a stick–slip mode. In continuous crack propagation the fracture energy is defined uniquely by the failure load, while in the stick–slip mode two values are definable – the so-called initiation energy,  $G_I$ , at the onset of crack jumping and the arrest energy,  $G_A$ .

Measurements were carried out on an Instron machine at constant cross-head speeds at temperatures between  $20$  and  $-196^{\circ}\text{C}$ . Low temperatures were attained by blowing cold nitrogen gas over the top and bottom surfaces of the specimen – the nitrogen gas being cooled by passage through a coil of copper tube immersed in liquid nitrogen. The top surface was cooled by blowing the gas through a perforated coil fixed above the specimen while the bottom surface was cooled by passing gas through the base itself and up and through holes drilled along its length. The temperature immediately above and below the specimen was measured by two thermocouples, the outputs from which were fed to a chart recorder, and testing was only carried out after the two traces had converged and remained at the required temperature for at least  $\frac{1}{2}$  min. Subsidiary experiments with a

Figure 1 The double torsion test.



specimen in which was embedded a thermocouple verified that the whole specimen reached the required test temperature. The recorder was calibrated after each test, and the accuracies of  $\pm 2^\circ \text{C}$  were attained.

### 3. Results

#### 3.1. Effect of curing agent and curing conditions

In order to determine the effect of curing conditions three pairs of plates were manufactured using ethylene diamine as the curing agent and the cure schedules:

1 h at  $60^\circ \text{C}$  + 1 h at  $160^\circ \text{C}$

1 h at  $60^\circ \text{C}$  + 1 h at  $120^\circ \text{C}$

1 h at  $60^\circ \text{C}$  + 1 h at  $80^\circ \text{C}$

Each pair consisted of one plate containing the stoichiometric proportion of EDA and the other containing only 90% this amount. Specimens were prepared from these plates and broken at  $19^\circ \text{C}$  at a range of cross-head speeds. The results are shown in Figs. 2 to 4 and demonstrate that lowering the

postcure temperature and decreasing the proportion of curing agent have a similar effect in lowering  $G_I$  and, to a lesser extent,  $G_A$ , and in moving the stick-slip/continuous transition to lower cross-head speeds. Clearly crack propagation is extremely sensitive to cure schedule and proportion of curing agent, and as a 10% change in proportion of curing agent corresponds to only a 0.8% change in weight of the resin/amine mix, great care is required in preparing epoxide materials for fracture experiments.

The effect of curing agent can be seen by comparing Figs. 2, 5 and 6 which show the variation of fracture energy with testing rate for resin cured with stoichiometric amounts of EDA, PDA and TDA under the standard curing condition of 1 h at  $60^\circ \text{C}$  and 1 h at  $160^\circ \text{C}$ . Increasing the molecular length of the curing agent very significantly increases the initiation energy but has little effect on the arrest energy. For easier comparison the fracture energies obtained at  $0.05 \text{ cm min}^{-1}$  are shown in Table III and compared with the values

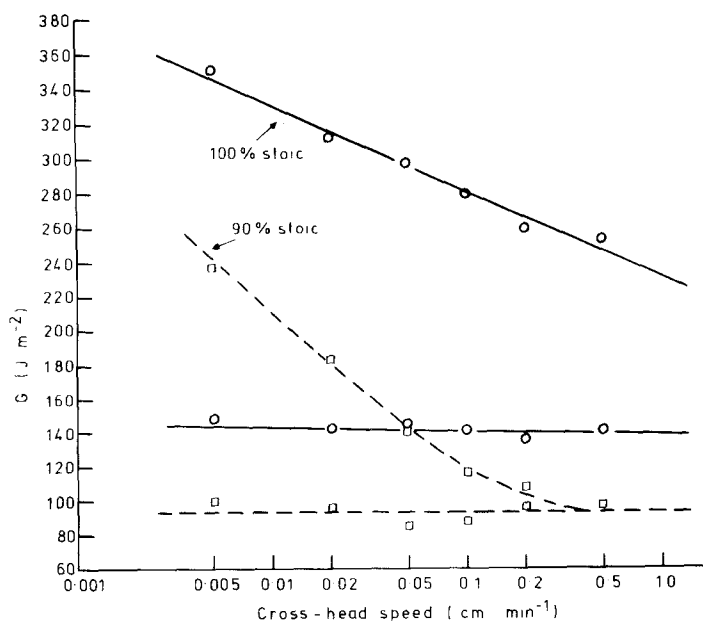


Figure 2 The variation of fracture energy with cross-head speed at  $19^\circ \text{C}$  for EDA-cured resin, post-cured at  $160^\circ \text{C}$ .

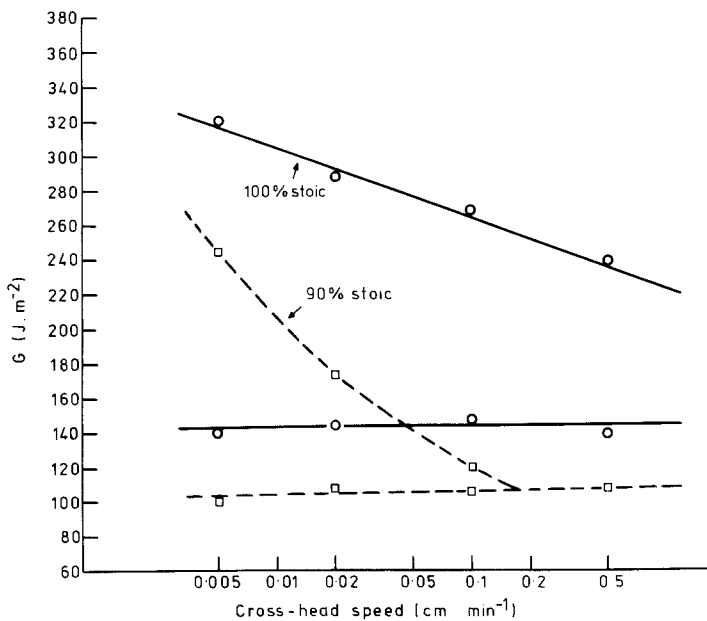


Figure 3 The variation of fracture energy with cross-head speed at 19° C for EDA-cured resin, post-cured at 120° C.

obtained in earlier work [1]. Fairly good agreement was obtained with the earlier data lending confidence in reproducibility.

### 3.2. Effect of water immersion

In investigating possible ways of cooling specimens, tests were carried out on specimens immersed in liquids. A marked effect occurred when specimens were immersed in water. Standard EDA-cured specimens which displayed stick-slip propagation in air at 19° C at all cross-head speeds were found, when immersed in distilled water at 19° C, to exhibit continuous crack propagation at low cross-head speeds. On increasing cross-head speed, the

load required, for continuous propagation increased until at 0.5 cm min<sup>-1</sup> a transition to stick-slip propagation occurred in water, as compared with a transition speed of less than 0.005 cm min<sup>-1</sup> in air.

### 3.3. Effect of testing temperature

Figs. 7 and 9 show the variation of fracture energy with testing temperature of EDA cured resin at 0.025, 0.25 and 1.25 cm min<sup>-1</sup>. On reducing temperature at the lowest cross-head speed, the expected transition from unstable to stable crack propagation occurs at about -16° C. On further reducing temperature crack propagation remains

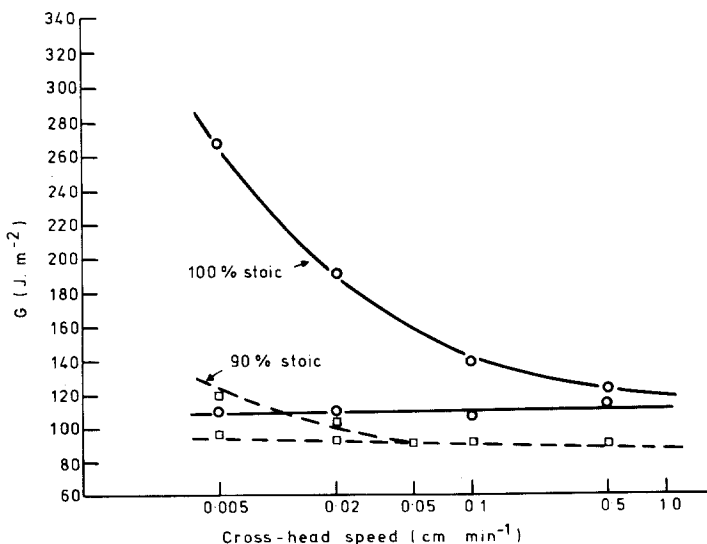


Figure 4 The variation of fracture energy with cross-head speed at 19° C for EDA-cured resin, post-cured at 80° C.

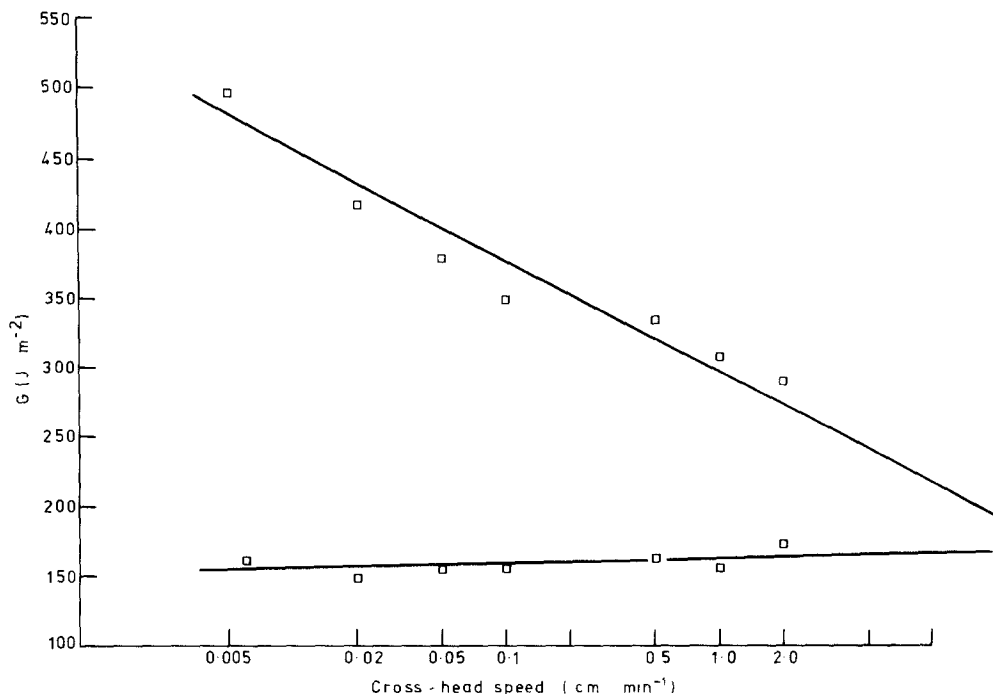


Figure 5 The variation of fracture energy with cross-head speed for PDA-cured resin at 19° C.

continuous with a slowly decreasing fracture energy down to approximately  $-140^{\circ}\text{C}$  when continuous propagation gives way to stick-slip. Similar behaviour occurs at  $0.25\text{ cm min}^{-1}$  but with the upper transition temperature increased to approximately  $4^{\circ}\text{C}$  and the lower transition temperature also being displaced to approximately  $-130^{\circ}\text{C}$ . At  $1.25\text{ cm min}^{-1}$  the behaviour is more

complex. On decreasing temperature there is a transition from stick-slip to continuous behaviour with the upper transition temperature increased to  $11^{\circ}\text{C}$ . On further reducing temperature crack propagation reverts to stick-slip in a zone extending from  $-20$  to  $-60^{\circ}\text{C}$ , changes to continuous between  $-60$  and  $-115^{\circ}\text{C}$  and then remains stick-slip to the lowest measured temperatures.

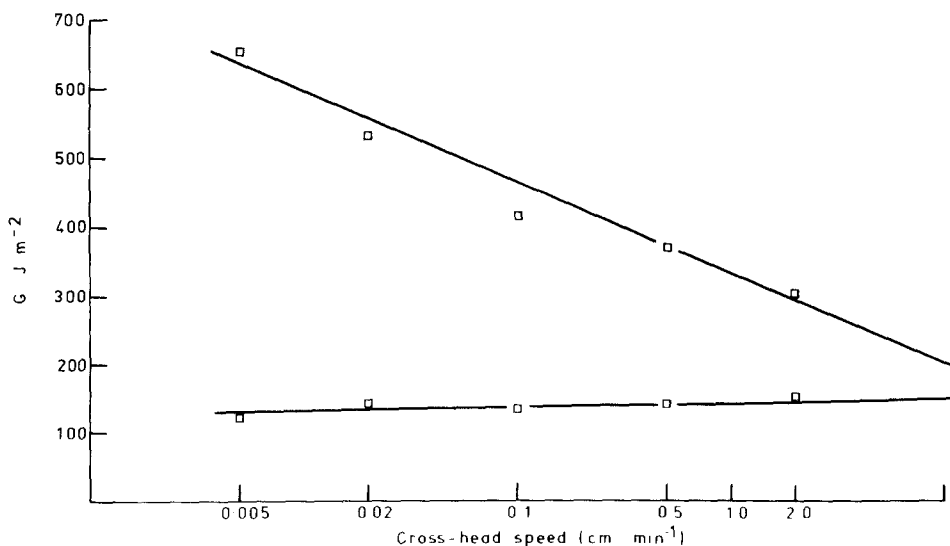


Figure 6 The variation of fracture energy with cross-head speed for TDA-cured resin at 19° C.

TABLE III Variation of fracture energy with curing agent  $\text{NH}_2(\text{CH}_2)_n\text{NH}_2$  at  $0.05 \text{ cm min}^{-1}$  and approximately  $20^\circ \text{ C}$ . Data in parentheses were obtained in earlier work [1]

Curing agent	Chain length parameter, $n$	Initiation energy $G_I(\text{Jm}^{-2})$	Arrest energy, $G_A(\text{Jm}^{-2})$
EDA	2	284 ( $329 \pm 38$ )	140 ( $164 \pm 19$ )
PDA	3	380	160
TDA	4	475 ( $489 \pm 83$ )	140 ( $160 \pm 20$ )
HDA	6	( $575 \pm 50$ )	( $155 \pm 14$ )

Results are also shown for TDA- and HDA-cured material in Figs. 10 and 11 obtained at the intermediate testing speed of  $0.25 \text{ cm min}^{-1}$ . The behaviour of the TDA-cured material is similar to that of the EDA material at the same testing rate but the HDA data more closely resembles that of the high testing rate EDA data.

The transitions from one mode of crack propagation to another on changing temperature were apparent also in changes in the shapes of the load-displacement (or time) traces obtained on the testing machine. A selection of load-displacement traces are illustrated in Fig. 12. These are copies of the actual charts from which were obtained the data on HDA-cured material at  $0.25 \text{ cm min}^{-1}$  shown in Fig. 11. Fig. 12a ( $8^\circ \text{ C}$ ) shows the typical

sharp peaks and troughs associated with crack jumping. As temperature decreases the initiation load decreases and the arrest load increases until they merge at the first transition to continuous propagation to give Fig. 12b ( $-37^\circ \text{ C}$ ). On further decreasing temperature there is a return to stick-slip behaviour as illustrated by Fig. 12c ( $-53^\circ \text{ C}$ ) which shows a series of high-speed unstable crack extensions initiated from an apparently stable propagating crack. This gives way to purely stick-slip propagation with sharp peaks and troughs as in Fig. 12d ( $-65^\circ \text{ C}$ ) down to  $-80^\circ \text{ C}$  at which point a transition to continuous propagation occurs typified by Fig. 12e ( $-88^\circ \text{ C}$ ). A rather ill-defined transition from stable to unstable propagation begins at approximately  $-130^\circ \text{ C}$  as shown by

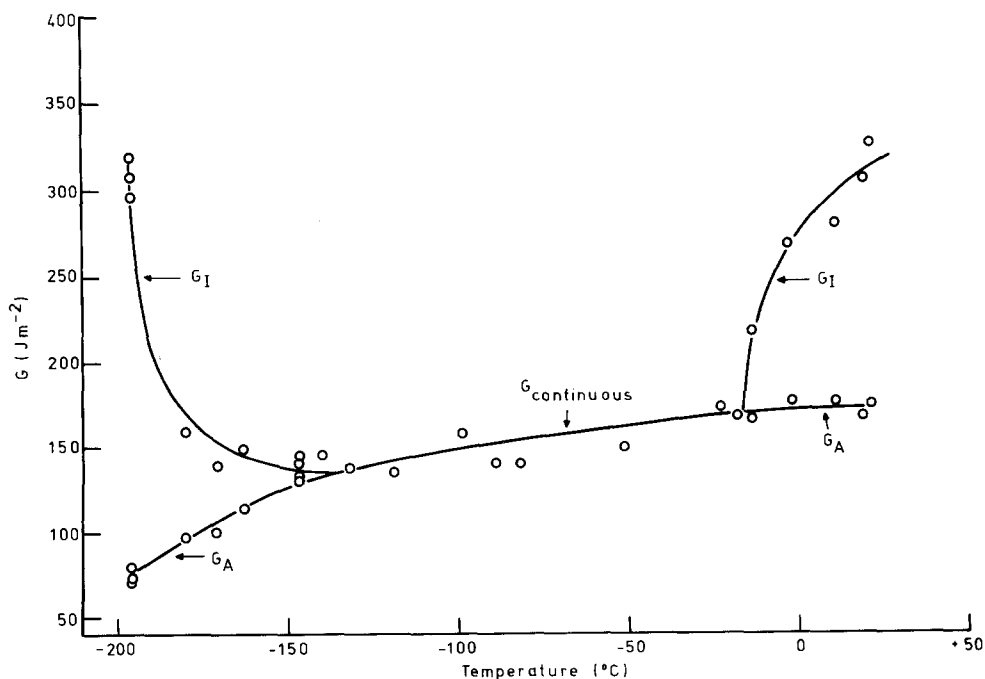


Figure 7 The variation of fracture energy with temperature for EDA-cured resin at a cross-head speed of  $0.025 \text{ cm min}^{-1}$ .

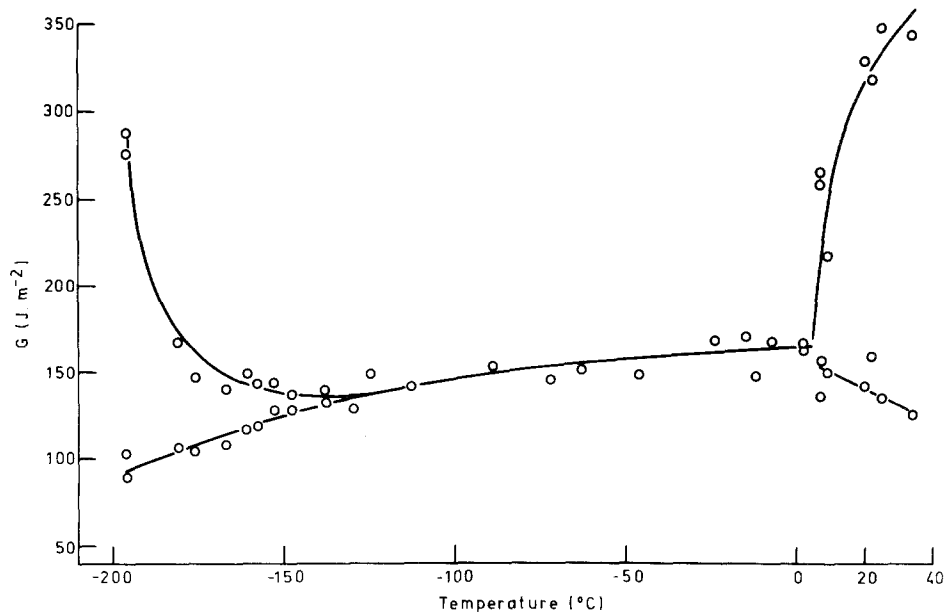


Figure 8 The variation of fracture energy with temperature for EDA-cured resin at a cross-head speed of  $0.25 \text{ cm min}^{-1}$ .

Fig. 12f ( $-133^\circ \text{C}$ ) – a reduction in temperature increasing the difference in initiation and arrest loads with a consequent increase in the length of crack jumps. Rounding-off of the peaks occurs down to  $-150^\circ \text{C}$  (Fig. 12g at  $-144^\circ \text{C}$ ) but below this temperature sharp peaks and troughs are formed (Fig. 12h at  $-174^\circ \text{C}$ ).

The effects of curing agent and testing rate on the high- and low-transition temperatures are summarized in Table IV. Increasing testing rate causes

an increase in both the transition temperatures, while increasing the curing agent, molecular length substantially reduces the upper transition temperature while not significantly altering the lower transition temperature.

The appearance of the fracture surfaces also varies significantly with testing temperature. Figs. 13 to 15 show a series of optical micrographs of fracture surfaces obtained from EDA-cured material tested at  $0.25 \text{ cm min}^{-1}$ . At temperatures

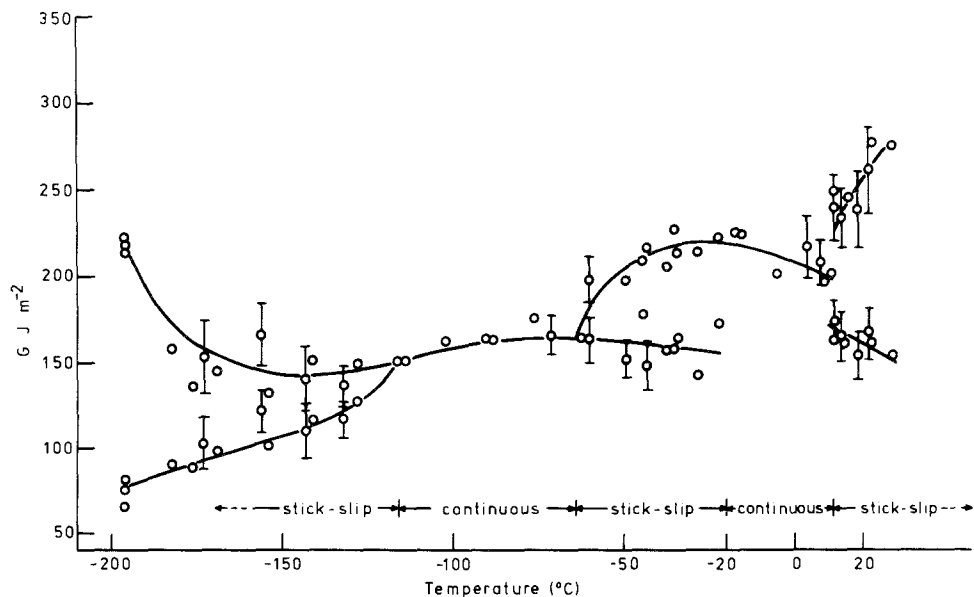


Figure 9 The variation of fracture energy with temperature for EDA-cured resin at a cross-head speed of  $1.25 \text{ cm min}^{-1}$ .



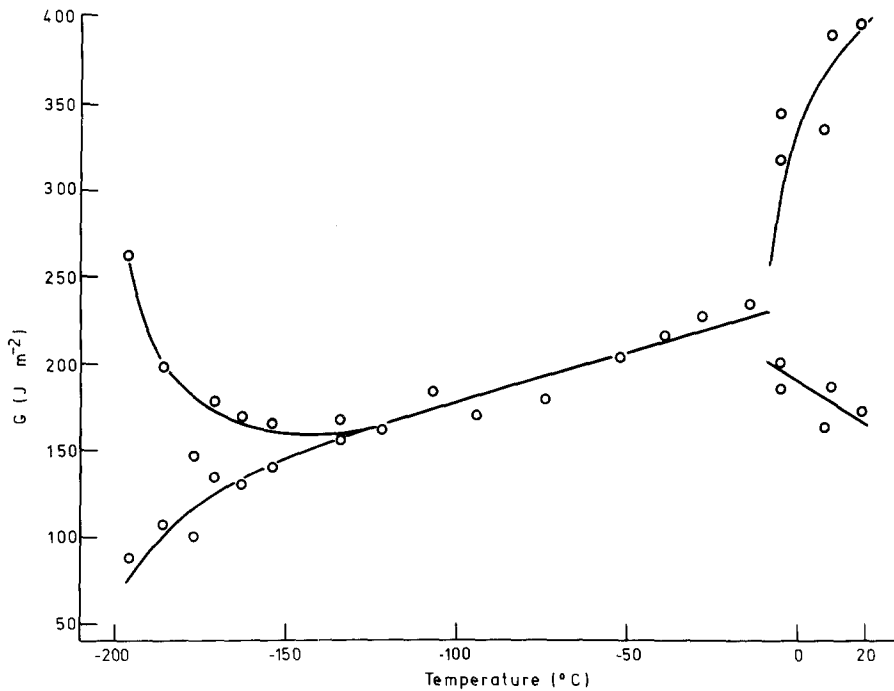


Figure 10 The variation of fracture energy with temperature for TDA-cured resin at a cross-head speed of 0.25 cm min<sup>-1</sup>

greater than the upper transition temperature the fracture surfaces display the characteristic markings associated with crack arrest which have been described previously [1]. Figs. 13a and b, for example, show crack arrest marks at 9° C. Previous work has shown that these features are associated with the crack abruptly arresting and then, on re-loading, slowly growing through the rough region

to finally accelerate away rapidly to produce the hackles. Slightly below the upper transition temperature the fracture surfaces were as shown in Fig. 14a and b for 2° C, with a rough surface at the top of the specimen. It must be recalled that with this specimen geometry the crack moves with different velocities along its front, velocity being highest at the tensile surface and lowest at the compression

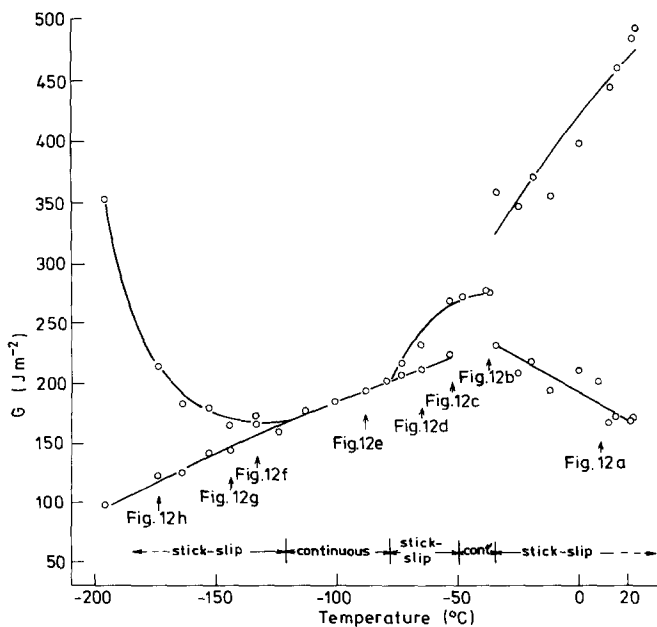


Figure 11 The variation of fracture energy with temperature for HDA-cured resin at a cross-head speed of 0.25 cm min<sup>-1</sup>.

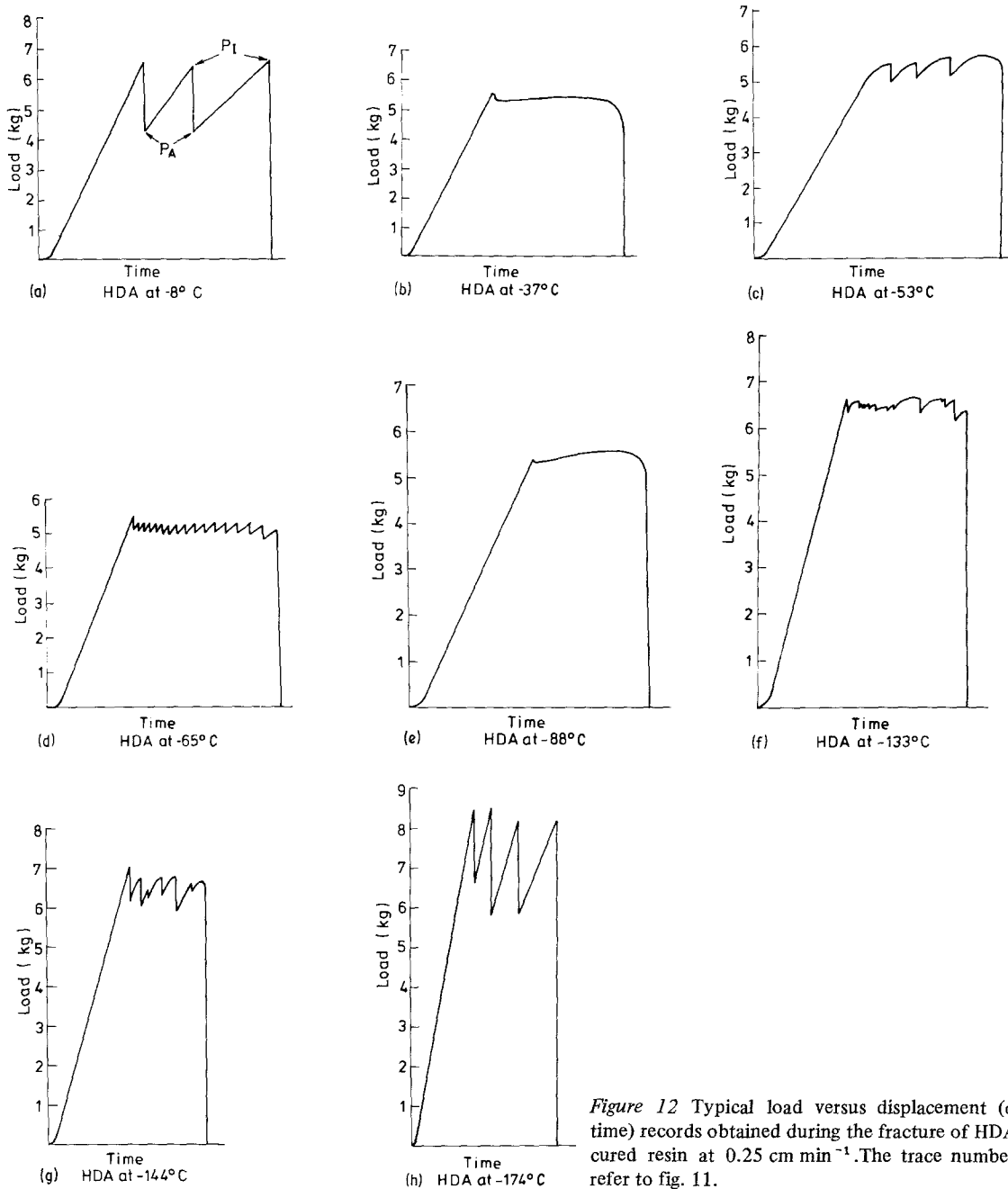


Figure 12 Typical load versus displacement (or time) records obtained during the fracture of HDA-cured resin at  $0.25 \text{ cm min}^{-1}$ . The trace numbers refer to fig. 11.

surface. At lower temperatures, in the continuous region, no surface features are apparent at the highest magnification possible with an optical microscope or in a scanning electron microscope. Finally, in the vicinity of the lower transition temperature, features become visible again and Figs. 15a and b obtained at  $-181^\circ \text{C}$  show their typical appearance.

#### 4. Discussion

The way in which fracture energy and mode of crack propagation of this epoxide resin vary with temperature depends both on testing rate and the molecular length of the curing agent. For all the curing agents and testing rates studied at least two transitions occur on cooling, a higher temperature transition ( $T_H$ ) at which the mode changes from

TABLE IV Variation of transition temperatures with curing agent and testing rate

Testing rate (cm min <sup>-1</sup> )	Transition Temperature (° C)					
	EDA		TDA		HDA	
	T <sub>H</sub>	T <sub>L</sub>	T <sub>H</sub>	T <sub>L</sub>	T <sub>H</sub>	T <sub>L</sub>
0.025	-15	-140				
0.25	4	-130	-10	-130	-35	-125
1.25	11	-115				

stick-slip to continuous and a lower temperature transition ( $T_L$ ) at which it reverts to stick-slip. Only these two transitions occurred in EDA-cured material at 0.025 and 0.25 cm min<sup>-1</sup> and TDA-cured material at 0.25 cm min<sup>-1</sup>. A more complicated sequence of events was exhibited by EDA-cured material at 1.25 cm min<sup>-1</sup> and HDA-cured material at 0.25 cm min<sup>-1</sup> in which further transitions to stick-slip and back to continuous occurred at temperatures between  $T_H$  and  $T_L$ . This suggests that these additional intermediate temperature transitions occur in a resin cured with a curing agent of given molecular length as the testing rate increases, or in a resin being tested at a given testing rate as the molecular length of the curing agent increases.

The upper transition  $T_H$  was expected, and was indeed the original object of this study, but the lower temperature transitions were unexpected and the reasons for their occurrence are not yet understood.

The reasons for the upper transition are

qualitatively understood and have been described earlier and outlined in section 1. A transition from stick-slip to continuous propagation occurs on decreasing temperature when the material at the crack tip is unable to deform plastically sufficiently rapidly to relieve the increasing stress. At temperatures greater than  $T_H$  the fracture initiation energy is largely controlled by the plastic flow behaviour of the resin. Table IV shows that  $T_H$  increases with increasing testing rate and decreases with increasing molecular length of curing agent. The increase of  $T_H$  with testing rate is to be expected. The flow of epoxides during yielding can be treated as a viscous flow mechanism and the yield stress  $\sigma_y$  of an epoxide resin increases with an increasing strain rate  $\dot{\gamma}$  and decreasing temperature according to an expression of the form

$$\dot{\gamma} = AT \exp \frac{\phi\sigma_y - U}{kT}$$

where  $\phi$ ,  $U$  and  $A$  are constants [1]. As strain rate is increased the yield stress will be increased, plastic deformation will be more limited and the tendency for stick-slip propagation to occur will decrease at that temperature. Thus  $T_H$  will be shifted to higher temperatures. As the molecular length of the curing agent is increased, the cross-linking density is expected to decrease. Table II shows that there is indeed a decrease in density associated with the more open structure and a consequential decrease in glass transition temperature and hardness which imply a tendency to easier viscous flow

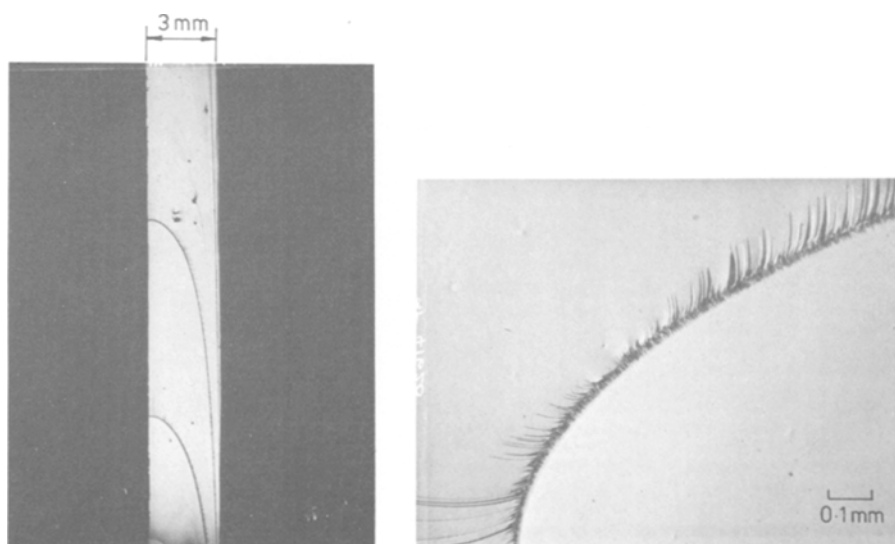


Figure 13 Fracture surface EDA at 0.25 cm min<sup>-1</sup> at 9° C.

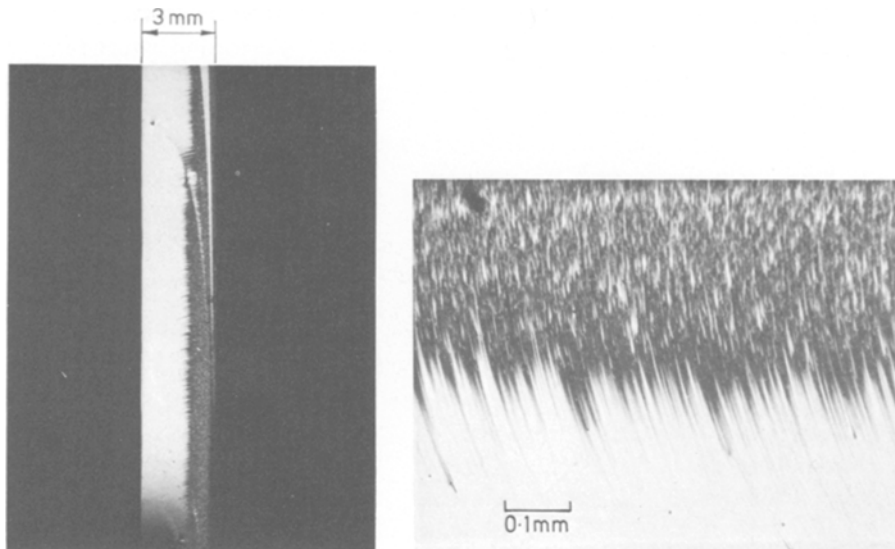


Figure 14 Fracture surface EDA at  $0.25 \text{ cm min}^{-1}$  at  $2^\circ \text{ C}$ .

of the material. Thus  $T_H$  would be expected to shift to low temperatures as the molecular length increases. The behaviour of  $T_H$  is thus consistent with the qualitative model proposed earlier.

This explanation, however, cannot be invoked to explain the lower transition temperature  $T_L$  as instability at low temperatures increased on decreasing temperature. The lower transition temperature increases with increasing strain rate but appears to be unaffected by curing agent. This lower transition is as yet not at all understood. Possible explanations may involve either an increase in damping capacity due to molecular relaxation

processes or else interaction of the material at the crack tip with its gaseous environment near the gas liquefaction temperature [6]. Both of these possibilities are currently being experimentally investigated.

The intermediate temperature transitions displayed in Figs. 9 and 11 are equally puzzling. It is possible that they are a result of the specimen geometry. Continuous crack propagation tends to occur when the fracture energy increases with increasing crack velocity, and stick-slip propagation when fracture energy decreases with increasing velocity. In a double torsion test the

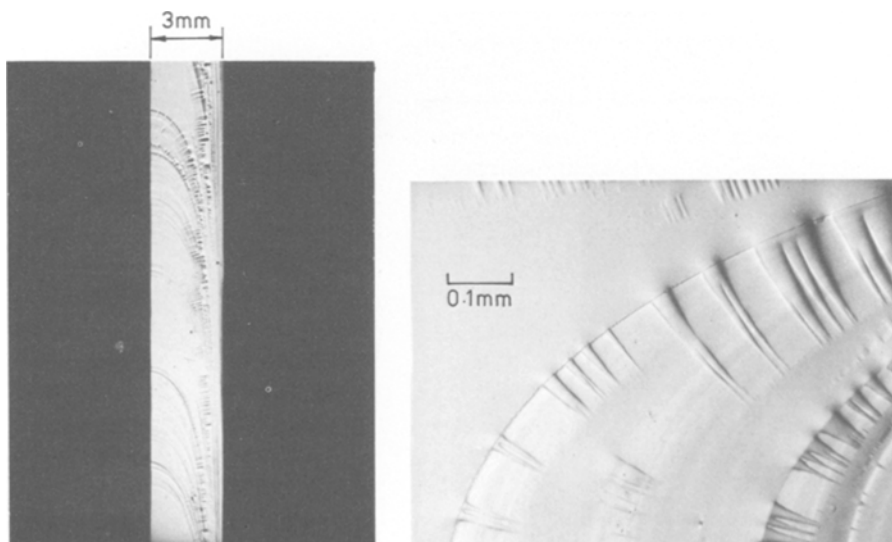


Figure 15 Fracture surface EDA at  $0.25 \text{ cm min}^{-1}$  at  $-181^\circ \text{ C}$ .

velocity of the crack varies along the crack front being a maximum near the tensile surface and a minimum near the compression surface. It is conceivable that the combination of the variation of  $G$  with crack velocity, and of crack velocity along the crack front could lead to conditions under which these intermediate transitions arise. This is supported by the appearance of the fracture surface in Fig. 14, which is rough in the region where the crack moves slowly but smooth in the region where it moves more rapidly.

The variation of appearance of fracture surface with temperature is significant. The features seen at temperatures above  $T_H$  have been reported before and have been shown to occur when a crack arrests abruptly and then grows slowly on reloading [1]. Below  $T_L$  the crack arrest marks are quite different, again supporting the idea that instability at low temperatures results from a different mechanism. To some extent they resemble the features seen on polyamine-cured resin fracture surfaces [1]. These have been shown to result from a crack decelerating relatively slowly prior to arrest and by comparison it seems possible that this is what occurs at low temperatures.

The effect of water on the transition from stable to unstable crack propagation observed in this work is also interesting. It appears that in this resin system at low cross-head speeds water can interact with the material at the crack tip to cause the crack to propagate stably instead of instably, but at high cross-head speeds there is insufficient time for this interaction to occur and the resin reverts to unstable crack propagation. This behaviour is the opposite to that observed by other workers [2].

## 5. Conclusions

Reduction of testing temperature induced a transition from stick-slip to continuous propagation. The variation of this upper transition temperature with molecular length of curing agent and testing

rate was consistent with the hypothesis of crack instability caused by viscous crack blunting.

With all resins and under all strain rates tested, a further transition from continuous to stick-slip propagation was apparent at approximately  $-150^\circ\text{C}$ . This low-temperature stick-slip region is not explicable by a simple crack blunting argument. Suggestions as to its cause include increased energy absorption by molecular relaxation processes, and interaction of the crack tip with the gaseous environment near its liquefaction temperature.

A stick-slip region at an intermediate temperature appeared under two specific combinations of testing rate and resin type. It is possible that this region arises as a result of the curved crack front produced by the double torsion configuration.

Crack propagation mode has been shown to be extremely sensitive to degree of cure. A decrease in curing agent concentration and lower postcure temperature acting in the same way to encourage continuous propagation.

## Acknowledgement

This article is published with permission of the UK Atomic Energy Authority (UKAEA) who retain copyright of the article.

## References

1. D. C. PHILLIPS, J. M. SCOTT and M. JONES, *J. Mater. Sci.* **13** (1978) 311.
2. S. YAMINI and R. J. YOUNG, *Polymer* **18** (1977) 1075.
3. J. M. SCOTT and D. C. PHILLIPS, unpublished work.
4. L. SCHECTER, J. SYNSTRA and P. KURKJY, *Ind. Eng. Chem.* **48** (1956) 94.
5. H. LEE and K. NEVILLE, "Handbook of epoxy Resins" (McGraw-Hill, New York, 1967).
6. Y. IMAI and N. BROWN, *J. Mater. Sci.* **11** (1976) 417.

Received 11 July and accepted 24 October 1979.